Journal of Computational and Applied Mathematics 477 (2026) 117202

Contents lists available at ScienceDirect

Journal of Computational and Applied Mathematics

journal homepage: www.elsevier.com/locate/cam

Numerical reconstruction of the kernel function in generalized non-convolutional fractional operators

Hamza Al-Shdaifat, Rosana Rodríguez-López *

CITMAga, Santiago de Compostela, 15782, Spain
Departamento de Estatística, Análise Matemática e Optimización, Facultade de Matemáticas, Universidade de Santiago de Compostela, Santiago de Compostela, 15782, Spain

ARTICLE INFO

Keywords:
Generalized fractional operators
Kernels
Numerical reconstruction

ABSTRACT

This paper deals with the numerical reconstruction of the kernel function $\kappa(t,z)$ for a new class of generalized non-convolutional fractional operators. These operators are defined in integral form of Volterra type and the general kernel is not always reducible to classical convolution-type expressions. The work focuses on the reconstruction of the kernel starting from the generalized Sonin condition, which connects the kernel of the integral operator with that of the corresponding differential operator.

Taking the generalized Sonin condition as the starting point, we propose a constructive numerical method by approximating the functional identity obtained from the integration of the product of both kernels, operation that is achieved by proper integration on segment lines of the domain. By casting the theoretical requirements as one-dimensional integral estimations on parameterized trajectories (segment lines), the problem becomes a nonlinear inverse problem for the determination of one of the kernels, κ, provided that the other one is known.

Our approach is based on the selection of a proper partition of the domain, and the consideration of the auxiliary functions $\varphi_{t,z}$ and $\phi_{t,z}$, which are combined in such a way that it is possible to compute the unknown functions $\psi_{t,z}$ and $\Psi_{t,z}$, provided that the given restrictions on the integrals in the generalized Sonin condition are fulfilled. The feasibility of reconstructing the kernel in some chosen test examples is illustrated by some numerical procedures, as a first step toward the implementation of generalized fractional models in numerical simulations, and also as a tool for the selection of proper kernels in the definition of generalized fractional operators.

1. Introduction and theoretical background

Fractional calculus has gained a significant attention in recent decades due to its ability to effectively model phenomena exhibiting memory effects, hereditary properties, and anomalous dynamics in a wide variety of scientific and engineering fields, including fluid dynamics, control theory, biological systems, and signal processing [1–5].

Classical fractional operators, primarily represented by the Riemann–Liouville and Caputo derivatives, are traditionally defined via convolution-type integrals characterized by power-law kernels. These classical definitions are widely used and firmly established but imply uniform memory structures and spatiotemporal homogeneity and have, thus, some obstacles in the application to more realistic situations arising in several current scientific and technological problems [5,6].

* Corresponding author at: Departamento de Estatística, Análise Matemática e Optimización, Facultade de Matemáticas, Universidade de Santiago de Compostela, Santiago de Compostela, 15782, Spain.
E-mail address: rosana.rodriguez.lopez@usc.es (R. Rodríguez-López).

https://doi.org/10.1016/j.cam.2025.117202
Received 30 June 2025; Received in revised form 17 September 2025
Available online 12 November 2025

To transcend such limitations, advances in fractional calculus over the past years have provided *generalized fractional operators* with kernels other than convolution-type and presenting varying or state-dependent integration limits [7,8]. This generalization makes the fractional calculus tools more versatile and applicable to complex models where memory effects have spatiotemporal non-uniform behaviors.

One of the most recent developments in this area has been provided by Al-Shdaifat and Rodríguez-López [9], who aimed to introduce a rigorous theoretical framework for fractional operators defined by general non-convolutional kernels. Their approach provides some fundamental theoretical contributions in this direction, such as the proposal of the operators, linearity properties, semigroup conditions, and a more comprehensive fundamental theorem of calculus, all these appropriate to generalized fractional operators that are not necessarily of convolution type. Despite these theoretical advances, significant challenges remain, particularly concerning the practical determination or numerical reconstruction of the kernel function $\kappa(t,z)$ from limited or indirect measurements. In particular, the generalized Sonin condition [9] establishes some necessary and sufficient identities that connect both corresponding kernels (those in the integral and the derivative operator, respectively).

Motivated by these challenges and recognizing the critical role played by an accurate kernel identification in applying generalized fractional models, this research aims to numerically reconstruct the kernel function $\kappa(t,z)$ for generalized non-convolutional fractional operators. This is the main motivation of our paper, i.e., the induction, by virtue of the generalized Sonin condition, of approximate values for the kernel of one of the fractional operators assuming the other one is known. This is essential for the definition of new generalized fractional operators, and to determine the derivative fractional operator that corresponds to a proposed generalized integral operator through the Sonin condition, which guarantees that certain relevant properties are fulfilled.

Specifically, our approach transforms integral-based theoretical constraints (generalized Sonin condition) into a tractable inverse problem framework. This is accomplished by constructing auxiliary functions $\varphi_{t,z}(u)$ and $\phi_{t,z}(u)$ defined along parameterized paths (segment lines) in the domain, thereby facilitating a systematic and robust numerical recovery process.

The numerical procedure explained in this work can possibly be applied to the study of the theory of transforms (see, for instance, [10]). Some connections of this process with the synchronization of neurons are also feasible [11]. Other possible future works might include the application of monotone iterative methods [12,13] in order to approximate solutions to the corresponding generalized fractional integral and differential problems.

The rest of the paper is organized as follows. Section 2 recalls the key classical fractional operators and compares them with the generalized fractional operators considered in this paper. To this purpose, we also recall the formulation of non-convolutional fractional operators proposed in [9], as well as the integral constraint (generalized Sonin condition) that will be needed later for the reconstruction of the kernel. Section 3 formulates the problem, presenting the details for the kernel reconstruction, and establishing the inverse strategy. Section 4 outlines the proposed numerical reconstruction scheme and applies it, including a detailed analysis of the results. Finally, Section 5 contains some concluding comments and research directions. Before passing to Section 2, we present a sketch of notation and terminology.

1.1. Notation and terminology

To maintain clarity and consistency, we define the relevant notation and terminology as follows:

- The triangular domain of interest is given by:

$$\Delta := \{(t,z) \in [0,1]\times[0,1] : z < t\}.$$

- The kernel of the integral operator is denoted by $\kappa : \Delta \to \mathbb{R}$.
- Parameterized paths used in the reconstruction are represented, respectively, by:

$$\gamma^{(1)}_{t,z}(u), \quad \gamma^{(2)}_{t,z}(u), \quad u \in [0,1].$$

- Auxiliary kernel-sampling functions along these paths are defined, respectively, as:

$$\varphi_{t,z}(u) = \kappa(\gamma^{(1)}_{t,z}(u), z), \quad \phi_{t,z}(u) = \kappa(t, \gamma^{(2)}_{t,z}(u)).$$

- Integral constraints involve weight functions denoted by:

$$\psi_{t,z}(u), \quad \Psi_{t,z}(u).$$

- The kernel reconstruction procedure is consistently termed a *two-dimensional inverse problem*.

An illustration of the domain and paths used is provided below in Fig. 1 (see Section 3.1).

2. Classical fractional operators

The classical theory of fractional calculus has its origins in the 17th century, but significant formal developments occurred during the 19th and 20th centuries through the relevant contributions of mathematicians such as Liouville, Riemann, Caputo, Grünwald, Letnikov, among others [1,2,14]. Fractional calculus extends the concept of integrals and derivatives to orders other than integers, permitting the description of processes with memory and hereditary properties inaccessible through normal integer-order calculus.

Two commonly used fractional derivative definitions are the *Riemann–Liouville derivative* and the *Caputo derivative*. They are both based upon the fractional integrals concept, but are vastly different in their treatment concerning initial conditions and the differentiability of functions.

The *Riemann–Liouville fractional integral* of order $\alpha > 0$ is defined as:

$$(I^{\alpha} f)(t) = \frac{1}{\Gamma(\alpha)} \int_0^t (t-\tau)^{\alpha-1} f(\tau)\, d\tau,$$

where $\Gamma(\cdot)$ denotes the Gamma function. Based on this integral, the *Riemann–Liouville fractional derivative* of order $\alpha > 0$ can be expressed by applying integer-order differentiation after fractional integration:

$$(D^{\alpha} f)(t) = \frac{d^n}{dt^n}(I^{n-\alpha} f)(t),$$

where $n = \lceil \alpha \rceil$. A notable challenge associated with the Riemann–Liouville derivative arises from its treatment of initial conditions, as it typically requires initial conditions involving fractional integrals, which are less intuitive from a physical or engineering perspective [1].

To address this difficulty, the *Caputo fractional derivative* modifies the order of integration and differentiation operations, placing differentiation inside the integral, as follows:

$$({}^{C}D^{\alpha} f)(t) = \frac{1}{\Gamma(n-\alpha)} \int_0^t (t-\tau)^{n-\alpha-1} f^{(n)}(\tau)\, d\tau.$$

Here, again, $n = \lceil \alpha \rceil$. The Caputo derivative provides great benefits in real-world model cases through the definition of the initial conditions in terms of integer-order classical derivatives, and, thus, it is well-positioned in physical and engineering applications like modeling the viscoelastic materials, control system models, and anomalous processes of diffusion [2,4].

As we observe, both fractional derivatives use convolution-type kernels in the form of $(t-\tau)^{\nu}$, with $\nu < 0$, naturally capturing the effects of power-law memory. Albeit widely applicable across various contexts, the classical kernels are very rigid in the case of more realistic situations entailing spatial or temporal inhomogeneities, varying memory patterns, or uneven dynamics [3,7]. Such built-in limitations are the strong motivation behind the development of more general and adaptive fractional operators, as described, for instance, in [9], from where we take the operators referred in the rest of this text.

In particular, we consider the left-sided general fractional integral and derivative of a function f, respectively, defined as:

$$({}_{l}I^{a}_{(\kappa)} f)(t) = \int_a^t \kappa(t,s) f(s) ds, \qquad a < t \le b, \tag{1}$$

$$({}_{l}D^{a}_{(k)} f)(t) = \frac{d}{dt} \int_a^t k(t,s) f(s)\, ds, \quad a < t \le b, \tag{2}$$

provided that they exist, where κ and k are certain kernels defined on Δ, and the corresponding notions for right-hand side operators. For the validity of several properties that are relevant in the theory of fractional calculus, we impose that the kernels κ and k are subject to the generalized non-convolution Sonin condition, consisting of the following two restrictions:

$$\int_z^t k(t,s)\kappa(s,z)\, ds = 1, \qquad (t,z) \in \mathring{\Delta}, \tag{3}$$

and

$$\int_z^t \kappa(t,s)k(s,z)\, ds = 1, \qquad (t,z) \in \mathring{\Delta}. \tag{4}$$

These identities will be relevant for the reconstruction of one of the kernels assuming that the other one is known, in order to define a properly coupled integral and derivative concepts.

3. Problem formulation and inverse model

In this section, we formulate the numerical inverse problem for reconstructing a bivariate kernel function $\kappa(t,z)$, which is fundamental in defining generalized non-convolutional fractional operators. Accurate reconstruction of such kernels is critical in effectively utilizing these operators in numerical simulations and theoretical analyses.

3.1. Domain and parameterized curves

We consider the above-mentioned triangular computational domain defined by:

$$\Delta := \{(t,z) \in [0,1] \times [0,1] : z < t\}.$$

Within the interior of this domain, we select two parameterized curves to systematically sample the kernel κ. These curves are deliberately chosen to simplify the integral constraints derived later, facilitating an efficient numerical treatment of the reconstruction problem.

Precisely, for each fixed reference point $(t,z) \in \mathrm{int}(\Delta)$, we define the following curves:

- **Curve 1 (Horizontal Segment):** varies the first argument from z to t:

$$\gamma_{t,z}^{(1)}(u) = t + (u-1)(t-z), \quad u \in (0,1),$$

with associated sampling function:

$$\varphi_{t,z}(u) = \kappa\big(\gamma_{t,z}^{(1)}(u),\ z\big). \tag{5}$$

- **Curve 2 (Vertical Segment):** varies the second argument from z up to t:

$$\gamma_{t,z}^{(2)}(u) = t - (1-u)(t-z), \quad u \in (0,1),$$

with associated sampling function:

$$\phi_{t,z}(u) = \kappa\big(t, \gamma_{t,z}^{(2)}(u)\big). \tag{6}$$

Fig. 1 visually illustrates these curves within the triangular domain Δ.

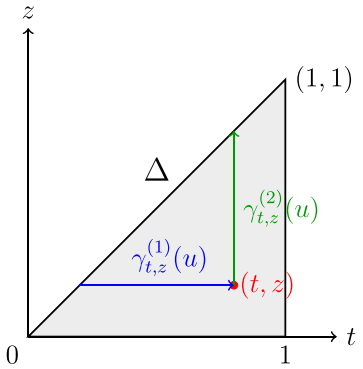

Fig. 1. Illustration of the triangular domain Δ and the parameterized curves used in reconstructing the kernel function $\kappa(t,z)$. The reference point (t,z) (in red) is used to define two sampling curves: a horizontal curve $\gamma_{t,z}^{(1)}(u)$ (in blue) and a vertical curve $\gamma_{t,z}^{(2)}(u)$ (in green).

3.2. Integral constraints and kernel reconstruction

To numerically reconstruct the kernel, we impose some integral constraints along the curves defined previously.

If we start from the integral operator, that is, if κ is known, then (5)–(6) are known, and we seek two families of weight functions, $\psi_{t,z}(u)$ and $\Psi_{t,z}(u)$, defined over the interval $(0,1)$, satisfying the following integral equations for all points $(t,z) \in \mathrm{int}(\Delta)$:

$$\int_0^1 \varphi_{t,z}(u)\,\psi_{t,z}(u)\,du = \frac{1}{t-z}, \tag{7}$$

$$\int_0^1 \phi_{t,z}(u)\,\Psi_{t,z}(u)\,du = \frac{1}{t-z}. \tag{8}$$

These weight functions allow to build a sampling of the kernel κ for the integral operator, or the kernel k of the derivative operator, respectively.

The integral constraints originate naturally from theoretical consistency conditions (generalized Sonin condition) required by the operators definition, in order for the integral operator to be left-inverse with respect to the derivative operator, imposing strong and physically meaningful restrictions on the kernel structure [9].

One relevant question is the existence and uniqueness of such weight functions. If we assume some regularity conditions, it is possible to derive these properties; however, in many cases, the assumed requirements include the continuity and boundedness of both the kernel and the weight function, which can be quite restrictive in practice.

Since this is a first attempt in this direction, we will assume quite restrictive conditions to illustrate the procedure. In this framework, the integral constraint paves the way for the solution of the problem of kernel reconstruction from a numerical point of view, which nurtures the foundations for a future rigorous theoretical development, but also serves as a practical illustration and visualization.

3.3. Establishment of the inverse problem

We have established a framework based on integral constraints, and the solution of the problem consists on the determination of the unknown weight functions, thus, to solve the problem is kind of equivalent to invert the constraints. In the study of the

generalized Sonin condition, we have two options: assume that the kernel κ is known, and try to obtain the kernel associated to the derivative, or start by assuming known the kernel associated to the derivative, and calculate the kernel κ associated to the integral operator. Since the constraints derived from the generalized Sonin condition are symmetric, we choose the second approach: we assume known the weight functions $\psi_{t,z}(u)$, and $\Psi_{t,z}(u)$ (totally or partially, just at certain points), and implement some method in order to recover the kernel $\kappa(t,z)$ of the integral operator.

The problem we have to address is, therefore, a two-dimensional inverse problem. In our case, the information is going to be recovered along the two one-dimensional curves $\gamma^{(1)}_{t,z}(u)$, and $\gamma^{(2)}_{t,z}(u)$ in the (t,z)-plane.

The solvability of the problem of interest is, normally, a tough task, due to the difficulty of the inversion. In this work, we present a numerical approach, with the help of a discretization of the integral constraints. However, the method is useful, at the moment, only for a restrictive class of kernels, since, to implement it, we require the hypotheses of continuity and boundedness on the kernel $\kappa(t,z)$. These assumptions are responsible for the well-posedness and numerical stability of the obtained system.

Property of nonlinearity for the inverse problem

In general, the integral identities (7)–(8) lead to the resolution of a nonlinear inverse problem. The simplest case is that where we assume fixed, known weight functions, so that the problem is reduced to solving a linear system for the unknown kernel $\kappa(t,z)$.

However, in practical applications, the weight functions often depend, directly or indirectly, on the kernel κ, introducing an inherent nonlinearity. These nonlinear relationships require the use of some iterative solution techniques, such as Newton-type or fixed-point methods, to approximate solutions effectively.

Moreover, inverse problems of this kind are typically ill-posed, meaning that even small perturbations in the input data or discretization can cause significant instability in the solution. Robust regularization techniques, such as Tikhonov regularization, are therefore essential to stabilize numerical solutions and ensure meaningful outcomes.

In this work, we begin with a simplified, linearized case using independent, predefined weight functions, leaving a deeper investigation of fully nonlinear scenarios for future research.

3.4. Discretization and system formulation

To numerically reconstruct the unknown kernel $\kappa(t,z)$ from the integral identities (7) and (8), we employ the following discretization procedure:

1. Discretize the interval $[0,1]$ into N subintervals with nodes $\{u_i\}_{i=1}^{N}$.
2. Approximate the integrals using numerical quadrature methods (e.g., the trapezoidal rule or Simpson's rule).
3. Formulate a discrete linear system linking the kernel values at the discretized points to the constraint $\frac{1}{t-z}$.

We define the vectors:

$$\mathbf{A}_{t,z} = \left[w_1\varphi_{t,z}(u_1),\ \dots,\ w_N\varphi_{t,z}(u_N)\right], \quad \mathbf{x}_{t,z} = \left[\psi_{t,z}(u_1),\ \dots,\ \psi_{t,z}(u_N)\right]^T,$$

and the scalar:

$$b_{t,z} = \frac{1}{t-z}.$$

This yields the linear system:

$$\mathbf{A}_{t,z}\,\mathbf{x}_{t,z} = b_{t,z}.$$

A similar discretization process is used for the second integral involving $\phi_{t,z}(u)$ and $\Psi_{t,z}(u)$. Once the constraints are compiled over a range of (t,z) points, the resulting system may become large and either linear or nonlinear. To ensure stable solutions, especially in the presence of ill-posedness, regularization strategies such as Tikhonov regularization are applied.

To make the reconstruction computationally tractable, we discretize both the integration variable u and the parameter set (t,z):

1. Divide the integration domain $[0,1]$ into N subintervals with nodes u_i and quadrature weights w_i.
2. Select M sample points (t_j,z_j), for $j=1,\dots,M$, in the interior of the domain.
3. For each sample (t_j,z_j), define:

$$A_j = [w_1\,\varphi_{t_j,z_j}(u_1),\ w_2\,\varphi_{t_j,z_j}(u_2),\dots,w_N\,\varphi_{t_j,z_j}(u_N)] \in \mathbb{R}^{1\times N},$$

$$x_j = [\psi_{t_j,z_j}(u_1),\psi_{t_j,z_j}(u_2),\dots,\psi_{t_j,z_j}(u_N)]^T \in \mathbb{R}^N,$$

$$b_j = \frac{1}{t_j - z_j} \in \mathbb{R}.$$

4. Assemble the global system:

$$A = \begin{pmatrix} A_1 \\ A_2 \\ \vdots \\ A_M \end{pmatrix}, \quad x = \left(x_1 \mid x_2 \mid \cdots \mid x_M\right), \quad b = \begin{pmatrix} b_1 \\ b_2 \\ \vdots \\ b_M \end{pmatrix}.$$

Each diagonal block $A_j x_j = b_j$ enforces the first integral constraint. We repeat the procedure similarly for the second constraint using ϕ_{t_j,z_j}, Ψ_{t_j,z_j} for the sample points (t_j, z_j). Note that we are not interested in a full system of the type $Ax = B$, since we are only taking the diagonal elements in the product matrix Ax.

5. Solve the combined linear system (with $2M$ equations in N unknowns) via regularized least squares.

Regularization (e.g., Tikhonov regularization) is then normally applied to stabilize the system against the inherent ill-posedness of inverse problems. We recall that ill-posedness for a problem consists on the lack of one of Hadamard's conditions (existence, uniqueness, or stability), in the sense that the problem might not have solutions, or it can have more than one solution, or the solution can differ significantly when the initial data is slightly modified.

3.5. Regularization for stability

Due to the above-mentioned inherent ill-posedness, directly solving a general linear system of the type

$$A\,\mathbf{y} = \mathbf{b}$$

can result in instability from data perturbations or discretization errors. To mitigate instability, we apply *Tikhonov regularization*, solving the minimization problem:

$$\min_{\mathbf{y}} \left(\left\| A\,\mathbf{y} - \mathbf{b} \right\|_2^2 + \lambda \left\| L\,\mathbf{y} \right\|_2^2 \right),$$

where:

- $\lambda > 0$ is the regularization parameter controlling the trade-off between data fidelity and solution smoothness.
- L is a regularization operator (often chosen as the identity operator I, or a finite-difference approximation for smoothing).

The resulting normal equations for this regularization problem are:

$$\left(A^T A + \lambda\, L^T L\right) \mathbf{y} = A^T \mathbf{b}.$$

Selection of λ. Common approaches include:

- *L-curve criterion*: Find a point of balance ('corner').
- *Generalized cross-validation* (GCV).
- *Discrepancy principle*: Choose λ based on estimated noise level.

We choose λ based upon the L-curve criterion and use $L = I$ (identity) in the numerical experiments, this way we obtain well-conditioned and convergent numerical systems.

Clarification on matrix dimensions

Remark 1. For each pair (t, z) fixed, the discretized integral constraint can be expressed in matrix form clearly following the scheme:

$$(1 \times N) \cdot (N \times 1) = (1 \times 1),$$

ensuring dimensional consistency and clarity in numerical implementations.

Impact of regularization. To illustrate the essential role of regularization, we have solved the inverse problem numerically with and without regularization ($N = 100$ nodes). Without regularization, solutions exhibited instability and significant oscillations. Applying Tikhonov regularization ($\lambda = 0.01$) stabilized solutions dramatically, reducing the relative error from approximately 10^{-2} to 10^{-4}.

4. Numerical implementation and validation

In this section, we translate the theoretical model developed in the above sections into a computational procedure. We aim to numerically validate the proposed reconstruction algorithm for the kernel function $\kappa(t, z)$ through controlled simulations. We detail the discretization method, numerical methods for the integrals, as well as the regularization methods employed for stability and accuracy of the solution. We further analyze the method performance in different cases, from smooth through non-smooth kernel cases, with emphasis laid, in particular, on regions where the inverse problem is found to be ill-conditioned. Such rigorous verification adds strength to the method, and it points toward its practical limitations, laying the ground for its application in real fractional modeling problems.

4.1. Numerical strategy

In order to apply the kernel reconstruction algorithm numerically, we discretize the integration domain as well as the parameter domain on which the kernel is sampled. The reconstruction is carried out through numerical quadrature for the approximation of the integral constraints, and the system of equations formed is solved through regularized least squares. In the following, we describe the procedure for discretization, the formation of the numerical system, and the choice of regularization parameters to guarantee the stability in the inversion process.

Quadrature on $[0, 1]$.

We begin by discretizing the integration domain $[0, 1]$ using a uniform grid of N equally spaced nodes $\{u_i\}_{i=1}^N$. For the numerical integration, we employ the trapezoidal rule, which balances simplicity and accuracy in approximating integrals of smooth functions. The quadrature nodes and weights are defined as follows:

$$u_i = \frac{i-1}{N-1}, \quad i = 1, 2, \dots, N,$$
$$w_1 = w_N = \frac{1}{2(N-1)}, \quad w_i = \frac{1}{N-1}, \quad \text{for } i = 2, \dots, N-1.$$

This discretization allows the integrals involving the sampling functions $\phi_{t,z}(u)$ and $\varphi_{t,z}(u)$ to be approximated efficiently for each selected point (t, z) in the domain.

Sampling in (t, z). To evaluate the kernel $\kappa(t, z)$ across the computational domain, we construct a uniform grid over the triangular region

$$\Delta = \{(t, z) \in [0, 1]^2 : z < t\}.$$

We select M sampling points $\{(t_j, z_j)\}_{j=1}^M$ such that the difference $t_j - z_j$ remains bounded away from zero to avoid numerical instability due to the singular behavior of the right-hand side term $1/(t - z)$.

In practice, we generate a grid over $[0, 1]^2$ and retain only those points satisfying $t_j - z_j \geq \epsilon$ for a small positive threshold ϵ (e.g., $\epsilon = 10^{-3}$). This ensures a stable evaluation of the integral constraints and avoids division by nearly zero values in the discrete system.

Assembly of the linear system. For each sampling point (t_j, z_j) in the interior of the domain Δ, we compute the discrete representation of the integral constraint using the previously defined quadrature nodes $\{u_i\}$, and weights $\{w_i\}$. Specifically, we evaluate the sampling function $\phi_{t_j,z_j}(u)$ at each quadrature node and form the corresponding row vector

$$A_j = \left[w_1 \, \phi_{t_j,z_j}(u_1), \, w_2 \, \phi_{t_j,z_j}(u_2), \, \dots, \, w_N \, \phi_{t_j,z_j}(u_N) \right] \in \mathbb{R}^{1 \times N}.$$

The right-hand side is defined as

$$b_j = \frac{1}{t_j - z_j},$$

and the resulting linear constraint takes the form

$$A_j x_j = b_j,$$

where $x_j \in \mathbb{R}^N$ is the discretized vector of the unknown weight function $\psi_{t_j,z_j}(u)$ evaluated at the quadrature nodes.

Stacking all M such equations yields a global linear system of the form

$$Ax = b,$$

where $A \in \mathbb{R}^{M \times N}$ is the matrix formed by the row vectors A_j, and $b \in \mathbb{R}^M$ is the vector of the corresponding right-hand sides. An analogous system is built using the second sampling function $\varphi_{t,z}(u)$ and the associated weight function $\Psi_{t,z}(u)$ to enforce the second integral constraint.

Regularization parameters. Due to the inherent ill-posedness of the inverse problem, directly solving the linear system $Ax = b$ may lead to unstable solutions, especially in the presence of noisy data or discretization errors. To mitigate this issue, we employ Tikhonov regularization by solving the following minimization problem:

$$\min_{x \in \mathbb{R}^N} \left(\|Ax - b\|_2^2 + \lambda \|Lx\|_2^2 \right),$$

where $\lambda > 0$ is the regularization parameter that controls the trade-off between fidelity to the data and smoothness of the solution, and L is the regularization operator. In this work, we choose $L = I_N$, the $N \times N$ identity matrix, which penalizes large norms of the solution vector x and encourages smoothness.

The normal equations for this regularized system are as follows:

$$(A^\top A + \lambda L^\top L)x = A^\top b.$$

We apply the *L-curve criterion* to choose a suitable value of λ, where the criterion finds a point of equilibrium between the solution norm $\|x\|_2$ and the residual norm $\|Ax - b\|_2$. We have observed in our experiments that the value $\lambda = 10^{-2}$ gives a good reconstruction both in terms of stability and accuracy over a wide range of test cases.

Implementation outline. The entire reconstruction algorithm is implemented in Python using the `NumPy` and `SciPy` libraries for efficient numerical computation and linear algebra operations. The main steps of the implementation are summarized as follows:

1. Generate the quadrature nodes $\{u_i\}_{i=1}^N$ and weights $\{w_i\}_{i=1}^N$ using the trapezoidal rule on the interval $[0, 1]$.
2. Construct a uniform grid of M sampling points (t_j, z_j) within the triangular domain Δ, excluding points where $t_j - z_j < 10^{-3}$.

Table 1
Validation of the kernel reconstruction using the analytical test case $\kappa(t, z) = \sin(\pi t)\cos(\pi z)$. The table reports exact and reconstructed values along with the absolute error at the selected sample points.

Point (t, z)	Exact $\kappa(t, z)$	Reconstructed	Absolute error
(0.2, 0.1)	0.5590	0.5587	3×10^{-4}
(0.4, 0.2)	0.4755	0.4751	4×10^{-4}
(0.6, 0.4)	0.1816	0.1814	2×10^{-4}
(0.8, 0.6)	−0.4755	−0.4753	2×10^{-4}
(0.9, 0.8)	−0.1816	−0.1814	2×10^{-4}

3. For each sample point (t_j, z_j):
   - Evaluate the sampling function $\phi_{t_j,z_j}(u_i)$ at each quadrature node u_i.
   - Assemble the row vector A_j and compute $b_j = 1/(t_j - z_j)$.
4. Stack the rows A_j into the matrix $A \in \mathbb{R}^{M\times N}$, and the values b_j into the vector $b \in \mathbb{R}^M$.
5. Solve the regularized normal equations:

$$(A^\top A + \lambda I_N)x = A^\top b,$$

   in order to get the discrete form of the kernel function.
6. Calculate the reconstruction error using the computed solutions and compare them with the available analytical solutions, where applicable.

This design strategy enables the reconstruction technique to be tested methodically across different kernels, and forms a flexible basis for extensions such as adaptive refinement and nonlinear inverse problem formulation.

4.2. Reconstruction results

In this part, we verify the suggested reconstruction technique using a synthetic kernel function whose analytical expression is known. This enables us to measure the accuracy and trustworthiness of the numerical technique via comparison of the reconstructed kernel values with the real ones.

We take the test case:

$$\kappa(t, z) = \sin(\pi t)\cos(\pi z),$$

which is continuously differentiable across the domain

$$\Delta = \{(t, z) \in [0, 1]^2 : z < t\}.$$

The weight functions used for the integral constraints are chosen as:

$$\psi(u) = 1 - u, \quad \Psi(u) = u.$$

For a set of representative points (t_j, z_j), we compute the numerical integrals:

$$I_j^{(1)} = \int_0^1 \phi_{t_j,z_j}(u)\,\psi(u)\,du, \quad I_j^{(2)} = \int_0^1 \varphi_{t_j,z_j}(u)\,\Psi(u)\,du,$$

and compare them to the theoretical values $b_j = 1/(t_j - z_j)$. The relative errors are reported to evaluate the effectiveness of the reconstruction. To generate the results reported in Table 1, we have selected five representative points (t, z) within the domain $\Delta = \{(t, z) \in [0, 1]^2 : z < t\}$ and applied the reconstruction algorithm using the analytical kernel $\kappa(t, z) = \sin(\pi t)\cos(\pi z)$. For each point:

- The exact kernel value $\kappa(t, z)$ was computed analytically.
- The sampling function $\phi_{t,z}(u) = \kappa(\gamma_{t,z}^{(1)}(u), z)$ was evaluated at $N = 100$ quadrature nodes $u_i \in [0, 1]$.
- The integral $\int_0^1 \phi_{t,z}(u)\psi(u)\,du$ was approximated using the trapezoidal rule with $\psi(u) = 1 - u$.
- The integral value was compared to the target value $1/(t - z)$, and the reconstructed kernel value was obtained by solving the corresponding linear system.
- Finally, the absolute error was computed as the difference between the reconstructed and exact values.

This step-by-step procedure has been repeated for each of the five sample points, allowing us to assess the accuracy of the method.

As shown in Table 1, the reconstructed values of the kernel $\kappa(t, z)$ closely match the exact analytical values at the selected sample points. The absolute errors remain below 5×10^{-4} in all cases, demonstrating a high degree of numerical accuracy. The findings verify the proposed reconstruction technique to work reliably with smooth kernel functions when $t - z$ takes moderate values. This concurrence also authenticates the strategy used in the implementation and the adopted regularization strategy.

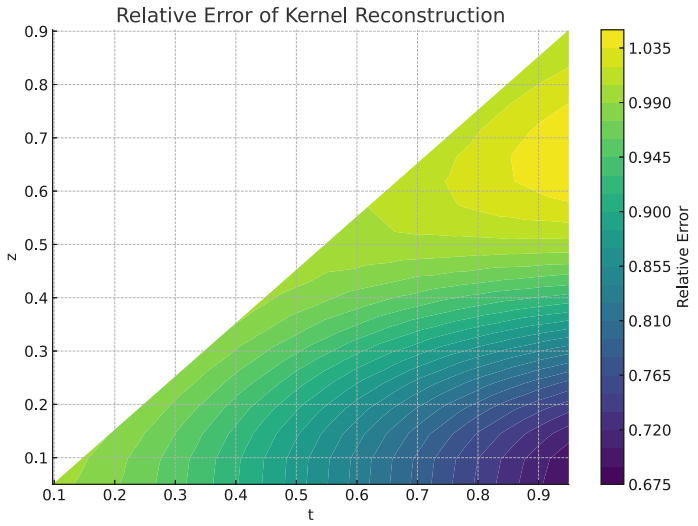

Fig. 2. Relative error of the reconstructed integral $\int_0^1 \phi_{t,z}(u)\,\psi(u)\,du$ over the triangular domain Δ using $N = 100$ quadrature nodes. Higher errors are observed near the diagonal, that is, for $t \approx z$, due to the singular behavior of the theoretical value $1/(t - z)$.

It is also noteworthy that the error does not exhibit any systematic bias and remains symmetrically distributed with respect to the sign of the kernel, suggesting numerical stability in both positive and negative regions of κ. These findings support the method's suitability for applications involving smooth, well-behaved kernels.

4.3. Analysis of the numerical behavior

To further understand the performance of the reconstruction method, we analyze its numerical behavior over a dense set of sampling points in the domain Δ. The objective is to assess both the accuracy and the stability of the method under varying geometric configurations of the input pair (t, z).

Specifically, we are concerned with the behavior of the reconstruction error when the size of the difference $t - z$ diminishes as the theoretical value $1/(t - z)$ converges toward a singularity. This type of region is particularly sensitive to discretization error and can become unstable. By sweeping the domain methodically, we measure the relative error in the reconstructed integrals and observe trends corresponding to kernel smoothness, sample density, and numerical regularization.

Fig. 2 shows the relative error over the domain. The reconstruction technique is accurate through the majority of the domain, and the relative error does not exceed 10^{-2} in well-separated (t, z) pairs. However, when $t - z \to 0$, the denominator $1/(t - z)$ gets large and magnifies any numerical and discretization errors, creating sharp spikes in the error. This vindicates the need to steer clear of, or regularize near-singularity configurations when doing reconstruction.

The results reveal several key aspects of the numerical behavior of the reconstruction method. First, the relative error remains uniformly low across the majority of the domain Δ, particularly when $t - z$ is moderately large. This indicates that the method performs well in reconstructing the kernel in regions that are not affected by singularity-driven instability.

Furthermore, the plot highlights the impact of the triangular domain's geometry: reconstruction is most stable in the central region, while instability grows toward the diagonal $t = z$. This observation supports the earlier decision to exclude sampling points with $t - z < 10^{-3}$ from the analysis to avoid numerical divergence.

In summary, the reconstruction algorithm exhibits strong numerical stability in well-separated (t, z) pairs, while requiring additional care or regularization in regions where the kernel evaluation approaches singularity. These insights will inform future adaptations of the method, including adaptive quadrature and region-specific regularization strategies.

4.4. Validation cases

To comprehensively validate the reconstruction algorithm, we apply it to two distinct test cases involving different types of kernel functions. The first case considers a smooth, infinitely differentiable kernel, while the second involves a piecewise-defined kernel that is continuous but non-differentiable at a specific point.

These contrasting scenarios allow us to assess the method's sensitivity to the kernel regularity, and to evaluate its robustness under both ideal and challenging conditions. For each case, we compare the reconstructed kernel values with the exact analytical expressions, and analyze the associated reconstruction errors across the domain.

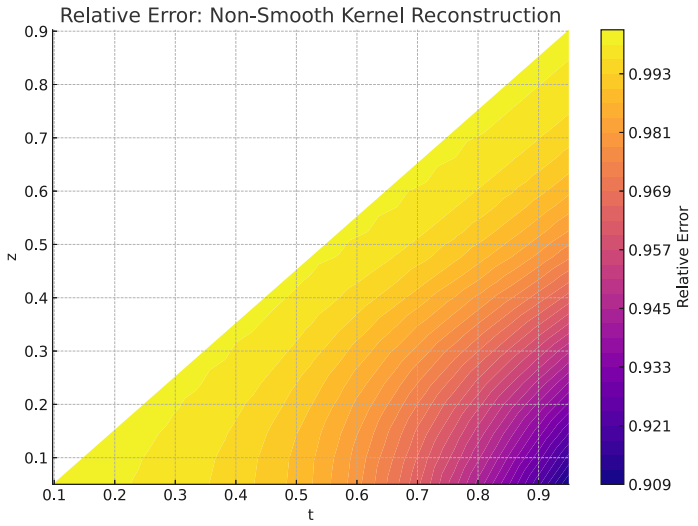

Fig. 3. Relative error of the kernel reconstruction for the non-smooth kernel defined in (9). Errors are notably higher near the transition point at $t = 0.5$, due to the lack of differentiability.

4.4.1. Case 1: Smooth kernel

To validate the reconstruction algorithm under ideal smoothness conditions, we consider the analytical kernel

$$\kappa(t, z) = \sin(\pi t)\cos(\pi z),$$

which is infinitely differentiable on the domain $\Delta = \{(t, z) \in [0, 1]^2 : z < t\}$. This test case, already analyzed in Section 4.2, demonstrates the accuracy and stability of the reconstruction method.

As shown earlier, the reconstructed values closely match the exact kernel values across several representative points, with absolute errors consistently below 5×10^{-4}. These results support the method's effectiveness when applied to smooth kernel functions.

4.4.2. Case 2: Non-smooth kernel

To assess the robustness of the reconstruction method under less favorable conditions, we consider a piecewise-defined kernel that remains continuous but is not differentiable when $t = 0.5$. The kernel is given by:

$$\kappa(t, z) = \begin{cases} t^2 - z^2, & \text{if } t < 0.5, \\ \sqrt{t} - \sqrt{z}, & \text{if } t \geq 0.5. \end{cases} \tag{9}$$

This example introduces a sharp transition in the smoothness of the kernel, challenging the reconstruction algorithm in terms of stability and accuracy.

We apply the same reconstruction procedure as in the smooth case, and compute the relative error over a grid of points $(t, z) \in \Delta$. The relative errors are visualized in Fig. 3, which shows that the reconstruction remains acceptable in most regions, but degrades near the transition boundary $t = 0.5$.

Fig. 3 illustrates the reconstruction error across the domain. While the method maintains reasonable accuracy in most regions, the error increases near the non-differentiable transition occurring at $t = 0.5$. This behavior is expected, as the approximation quality is sensitive to the kernel regularity, and sharp changes in smoothness introduce localized numerical instability.

Despite this degradation, the method still produces acceptable approximations away from the transition, highlighting its robustness under non-ideal conditions. This test emphasizes the importance of kernel smoothness in achieving high reconstruction accuracy and motivates further investigation into adaptive refinement or regularization strategies for non-smooth scenarios.

Comparison and insights

The two validation cases provide some contrasting perspectives on the influence of the kernel smoothness on the reconstruction accuracy:

- **Smooth Kernel:** The test case with $\kappa(t, z) = \sin(\pi t)\cos(\pi z)$, being infinitely differentiable, yielded highly accurate results with absolute errors consistently below 5×10^{-4}. The reconstruction closely matched the exact values across the domain, confirming the method's strength under ideal conditions.
- **Non-Smooth Kernel:** However, when considering a piecewise kernel with regions where it lacks differentiability, we find some areas with elevated error, this obstacle is especially acute when approaching the line where differentiability is not satisfied. In spite of that, the results remain quite acceptable and the method seems to be stable at some subdomains where the kernel is smooth, although the quality of the reconstructed data is poorer near the transition zone.

According to these remarks, we infer that the regularity of the kernel is essential for the good behavior of the computations over the whole domain, but does not prevent from getting accurate reconstructions of the kernel at subdomains that are far from the non-smooth region. The method has proved to perform robustly even when we consider non-differentiable kernels, but it is clear that the results improve considerably when taking smooth kernels. The examples used in this paper to illustrate the procedure are a motivation to explore some possible improvements in the future, maybe applying some adaptive refinement in the zones close to the non-differentiability region, or some other regularization strategies for rough kernels.

5. Conclusion

In this work, we have presented a numerical framework useful to reconstruct the value of a kernel function $\kappa(t, z)$ from an integral expression, which is applicable to the determination of kernels associated with generalized non-convolutional fractional operators in terms of the verification of the generalized Sonin condition [9]. The method is based on the reformulation of the integral restraints (consistency conditions of Sonin type) in terms of an inverse problem, and the determination of the (approximate) solution by using the numerical quadrature method and Tikhonov regularization.

In particular, we have taken the generalized Sonin condition as the starting point, and we have proposed a constructive numerical method with the aim of approximating the functional identities through a process of integration on segment lines of the domain. Considering these parameterized trajectories, the problem is translated into an inverse problem for the determination of one of the kernels, κ, provided that the other one is known.

We have developed the corresponding numerical experiments, deducing that the reconstruction method provides highly accurate results if the kernel is smooth enough, observing absolute errors on the order of 10^{-4}, for the example provided. The case where the kernel is non-differentiable is more difficult to handle, but, even in this scenario, we have illustrated with an example that the accuracy of the method is acceptable in a considerably wide region of the domain. The errors behave considerably well even in this case, except near the region of non-differentiability, where their magnitudes increase.

After a careful observation of the behavior across the domain, we have noticed the sensitivity of the method near the diagonal (in practice, when $t \approx z$). This is because the diagonal is the place where a theoretical singularity appears (due to the term $1/(t-z)$), so that the discretization errors are amplified. However, when moving apart from these singularities, the algorithm proposed seems to present robustness and stability.

The process presented for the reconstruction of the kernel starting from the generalized Sonin condition is an essential step to establish connections between generalized fractional integral operators and the corresponding differential operators.

Future Work. As this is our first attempt to address the problem of determining kernels that are correspondent through the integral restraints considered, there are several promising directions which still arise:

- One possibility is to investigate the usefulness of some adaptive quadrature techniques that allow us to refine the integration near the regions of non-regularity of the kernel.
- It would be also interesting to develop some regularization strategies in order to handle the possible irregularities of the kernel.
- Some more general problems can be considered, extending, thus, the method to fully nonlinear inverse problems, allowing the situation where the weight functions depend on the kernel.
- An always relevant question is to apply this type of study to some real-world problems whose models exhibit memory-dependent dynamics, since the motivation of the work is precisely the analysis of the correspondence between kernels in different types of fractional operators, and these operators are important, for instance, in the study of anomalous diffusion models, or viscoelastic systems.

Overall, with this study, we have tried to start the foundations for a numerical treatment of the integral constraints related to generalized fractional integral and differential operators, opening also a door to further advancements in the applications of inverse problems in the theory of fractional calculus.

Funding

This research was partially supported by the Agencia Estatal de Investigación (AEI) of Spain, co-financed by the European Fund for Regional Development (FEDER) corresponding to the 2021–2024 multiyear financial framework, project PID2020-113275GB-I00, and ED431C 2023/12 (GRC Xunta de Galicia).

Declaration of competing interest

The authors declare that they have no known competing financial interests or personal relationships that could have appeared to influence the work reported in this paper.

Acknowledgments

We thank the Editor and the anonymous Referees for their interesting and helpful comments and suggestions toward the improvement of the manuscript.

Data availability

No data was used for the research described in the article.

References

[1] I. Podlubny, Fractional Differential Equations, Academic Press, 1999.
[2] A.A. Kilbas, H.M. Srivastava, J.J. Trujillo, Theory and Applications of Fractional Differential Equations, Vol. 204, Elsevier, 2006.
[3] F. Mainardi, Fractional Calculus and Waves in Linear Viscoelasticity: An Introduction To Mathematical Models, World Scientific, 2010.
[4] J. Sabatier, O.P. Agrawal, J.A.T. Machado, Advances in Fractional Calculus, Springer, 2007.
[5] R.L. Magin, Fractional Calculus in Bioengineering, Begell House Publishers, 2006.
[6] R. Hilfer, Applications of Fractional Calculus in Physics, World Scientific, 2000.
[7] V.E. Tarasov, Fractional Dynamics: Applications of Fractional Calculus To Dynamics of Particles, Fields and Media, Springer, 2011.
[8] M.D. Ortigueira, Generalized Fractional Calculus and Applications, Springer, 2015.
[9] H. Al-Shdaifat, R. Rodríguez-López, Non-convolutional general fractional operators and some of their properties, J. Comput. Appl. Math. 464 (2025) 116527, http://dx.doi.org/10.1016/j.cam.2025.116527, https://www.sciencedirect.com/science/article/pii/S0377042725000421.
[10] N. Jiang, Q. Feng, X. Yang, J.-R. He, B.-Z. Li, The octonion linear canonical transform: properties and applications, Chaos Solitons Fractals 192 (2025) 116039, http://dx.doi.org/10.1016/j.chaos.2025.116039.
[11] H. Tian, J. Wang, J. Ma, X. Li, P. Zhang, J. Li, Improved energy-adaptive coupling for synchronization of neurons with nonlinear and memristive membranes, Chaos Solitons Fractals 199 (2025) 116863, http://dx.doi.org/10.1016/j.chaos.2025.116863.
[12] B. Hu, Y. Liao, Convergence conditions for extreme solutions of an impulsive differential system, AIMS Math. 10 (5) (2025) 10591–10604, http://dx.doi.org/10.3934/math.2025481.
[13] Y. Li, Z. Rui, B. Hu, Monotone iterative and quasilinearization method for a nonlinear integral impulsive differential equation, AIMS Math. 10 (1) (2025) 21–37, http://dx.doi.org/10.3934/math.2025002.
[14] S.G. Samko, A.A. Kilbas, O.I. Marichev, Fractional Integrals and Derivatives: Theory and Applications, CRC Press, 1993.